

# Development of a Constitutive Model to Describe the Dynamic Response of Soft Submarine Clay Deposits

T. Anantanavanich, J.M. Pestana & B.D. Carlton

*University of California, Berkeley*



## SUMMARY:

Submarine landslides triggered by earthquakes pose one of the greatest threats to offshore facilities such as pipelines, oil platforms, and communication cables. In addition, the large amount of material involved in such landslides can cause devastating tsunamis. The assessment of seismic performance and estimation of permanent displacements for submerged slopes requires the accurate description of a soil's stress-strain-strength relationship under irregular cyclic loading. This paper describes the formulation of a simplified effective-stress-based model, referred to as the MSimpleDSS model, which is able to capture the key aspects of the cyclic behavior of normally consolidated to slightly overconsolidated clays on level and sloping ground. The model has seven input parameters, and is formulated such that each material parameter has a clear meaning to assure simple and unique estimation. The parameters can be determined from one standard monotonic simple shear test and one cyclic simple shear test.

*Keywords: Constitutive laws, submerged slopes, clays, cyclic behavior*

## 1. Introduction

Submarine landslides are capable of transporting sediment as far as hundreds of kilometers and involving thousands of cubic kilometers of material (e.g., Storegga Slide, Bugge et al. 1988). As a result, submarine slope instability is considered to be one of the most serious threats to offshore installations such as communication cables, pipelines, production wells, and oil platforms. Submarine slides can also trigger significant tsunamis with devastating consequences for coastal infrastructure. The ability to estimate the deformations and excess pore pressures developed during seismic loading of submarine slopes is therefore crucial to evaluating the risk at a particular location.

For modeling purposes, the problem of site response of submarine slopes can be simplified to the solution of one-dimensional shear wave propagation in an infinite slope. The stress history is best simulated in the laboratory using the multidirectional simple shear (MDSS) device which is described extensively in the literature (e.g., Boulanger et al. 1991).

The scope of this research work is to develop a framework to model the response of normally consolidated to lightly overconsolidated clay deposits subjected to multidirectional seismic excitation. In order to achieve this goal, the constitutive model SimpleDSS (Pestana et al. 2000; Biscontin 2001) was improved. The SimpleDSS model developed by Pestana and Biscontin is a rate-independent model that describes the monotonic and cyclic behavior of lightly overconsolidated cohesive soils as observed in undrained simple shear tests. The model uses the concept of normalized material response, which is equivalent to that predicted by most effective stress models based on the Critical State Mechanics Framework (e.g., Roscoe and Burland 1968; Schofield and Wroth 1968).

The new MSimpleDSS model addresses several shortcomings of the previous model. First, under monotonic multidirectional shearing, the SimpleDSS model describes the relationship between

changes in shear stress ratio versus incremental shear strain in each direction independently. This type of formulation does not allow redistribution of the shear stresses between two directions. Second, for stress-controlled cyclic loading tests the SimpleDSS model cannot adequately capture the dependence of pore pressure development as a function of cyclic stress ratio (CSR). Finally, the SimpleDSS model defines the reversal point in strain space simultaneously in two directions. This means that both directions increase their stiffness to the initial stiffness ( $G_{max}$ ) regardless of the direction of the subsequent incremental strain in each direction. Therefore, the criteria in defining reversal points needs to be re-evaluated for multidirectional cyclic loading.

## 2. MODEL FORMULATION

The MSimpleDSS model is an effective stress soil model developed to predict the behavior of clay under  $K_o$  (level ground) and  $K_a$  (sloping ground) conditions. The following sections describe the mathematical development of the model.

### 2.1. Modeling monotonic response

#### 2.1.1. Pore pressure generation

The typical stress state of a soil element during an MDSS test is similar to that of a soil element on an infinite slope. The effective stress path during a monotonic MDSS test can be described by the Plastic State Surface (PSS) defined in the normal effective stress-shear stress ( $\sigma_n, \tau$ ) space as follows:

$$f_e = \eta^2 - \tan^2\psi + (\tan^2\psi + \eta_c^2 - 2\eta_c * \eta) \left[ \frac{\left(\frac{\sigma_n}{\sigma_p}\right)^m - \beta^m}{1 - \beta^m} \right] = 0 \quad (2.1)$$

$$\text{for } \beta < \frac{\sigma_n}{\sigma_p} < 1 \quad \eta = \begin{pmatrix} \tau_x/\sigma_n \\ \tau_y/\sigma_n \end{pmatrix} = \begin{pmatrix} \eta_x \\ \eta_y \end{pmatrix} \quad \eta_c = \begin{pmatrix} \tau_{xc}/\sigma_p \\ \tau_{yc}/\sigma_p \end{pmatrix} = \begin{pmatrix} \eta_{xc} \\ \eta_{yc} \end{pmatrix}$$

Where  $\tau_x$  and  $\tau_y$  are the shear stresses in the  $x$  and  $y$  directions,  $\sigma_n$  is the normal effective stress,  $\sigma_p$  is the maximum experienced normal effective stress,  $\eta$  is the shear stress ratio vector,  $\eta_c$  is the consolidation shear stress ratio vector, and  $\psi$ ,  $\beta$ , and  $m$  are material parameters described in section 3. The MSimpleDSS model has the same assumptions as its predecessor model in that the strength of soil at large strain can be described by critical state failure criteria, while the plastic response during shearing is controlled by the PSS. In other words, the undrained shear strength is controlled by the shape and orientation of the PSS, while large strain conditions are considered to be independent of previous straining history. The critical state failure conditions are represented by an isotropic conical surface with an aperture size equal to the shear stress ratio at failure ( $\tan \psi$ ). The PSS is terminated when it intersects with the failure cone and large strain failure conditions are established (see Figure 3.1).

#### 2.1.2. Stress-strain relationship

During shearing soils undergo both elastic and plastic deformations simultaneously. The MSimpleDSS model assumes that the elasticity of clay is linear and isotropic while the nonlinearity and anisotropy are controlled by the plasticity component of the model. For simplicity, the stress-strain response is described in terms of the change of shear stress ratio,  $\delta\eta$ , as a function of changes in shear strain,  $\delta\gamma$ .

The changes in shear stress ratio are related to the elastic strain component by the elastic shear modulus,  $G_e$ , given in Eqn. 2.2a.  $G_e$  is defined as the initial slope of the loading and unloading portion of the stress-strain curve and is a function of the effective normal stress as defined in Eqn 2.2b.

$$\begin{pmatrix} \delta\gamma_x^e \\ \delta\gamma_y^e \end{pmatrix} = \frac{1}{G_e} + \begin{pmatrix} \delta\eta_x \\ \delta\eta_y \end{pmatrix} \quad (2.2a)$$

$$G_e = G_n \left(\frac{\sigma_p}{\sigma_n}\right)^{1-b} \quad (2.2b)$$

Where  $b \cong 0.5$ ,  $G_n = G_{maxNC}/\sigma_p$ , and  $G_{maxNC}$  is the small strain shear modulus for normally consolidated conditions. For simplicity, the increment of plastic shear strains for the first loading

during multidirectional shearing is determined from the PSS as if it were the yield surface, defined in Eqn. 2.3, in which  $H$  is the plastic modulus and  $i = (i_x, i_y)$  = the unit outward normal vector to the PSS defined in Eqn. 2.4. The direction of  $i$  can be determined by differentiating Eqn. 2.1.

$$\begin{pmatrix} \delta\gamma_x^p \\ \delta\gamma_y^p \end{pmatrix} = \frac{1}{H} (i_x \delta\eta_x + i_y \delta\eta_y) \begin{pmatrix} i_x \\ i_y \end{pmatrix} \quad (2.3)$$

$$i = \frac{1}{\left[ \left( \frac{\delta f_e}{\delta \eta_x} \right)^2 + \left( \frac{\delta f_e}{\delta \eta_y} \right)^2 \right]^{1/2}} \begin{pmatrix} \frac{\delta f_e}{\delta \eta_x} \\ \frac{\delta f_e}{\delta \eta_y} \end{pmatrix} \quad (2.4)$$

This equation implies that the plastic modulus,  $H$ , is the tangent modulus of shear stress and plastic shear strain for the first loading which can be written as:

$$H = G_p \frac{\tan\psi - \sin(\eta_c \cdot \dot{\gamma}) \|\eta_c\|}{\|\eta - \eta_c\|} [\tan\psi - \sin(\eta_c \cdot \dot{\gamma}) \|\eta\|] \quad \text{for } \|\eta\| \leq \tan\psi \quad (2.5a)$$

$$H = \left\{ \left[ G_p \frac{\tan\psi - \sin(\eta \cdot \dot{\gamma}) \eta}{\tan\psi} \right]^{-1} - \frac{1}{G_e} \right\}^{-1} \quad \text{for } \|\eta\| > \tan\psi \quad (2.5b)$$

$$\sin(\eta_c \cdot \dot{\gamma}) = \begin{cases} 1 & \text{if } \eta_c \cdot \dot{\gamma} > 0 \\ 0 & \text{if } \eta_c \cdot \dot{\gamma} = 0 \\ -1 & \text{if } \eta_c \cdot \dot{\gamma} < 0 \end{cases} \quad (2.5c)$$

Where  $\|\eta\| = \sqrt{\eta_x^2 + \eta_y^2}$   $\|\eta - \eta_c\| = \sqrt{(\eta_x - \eta_{cx})^2 + (\eta_y - \eta_{cy})^2}$

and  $G_p$  is the material parameter that controls the shape of the back bone curve for normally consolidated soil. From Eqns. 2.2 and 2.3 the incremental stress-strain relations are expressed as:

$$\begin{pmatrix} \delta\eta_x \\ \delta\eta_y \end{pmatrix} = \frac{G_e^2}{G_e + H} \begin{bmatrix} \frac{H}{G_e} + i_y^2 & -i_x i_y \\ -i_x i_y & \frac{H}{G_e} + i_x^2 \end{bmatrix} \begin{pmatrix} \delta\gamma_x \\ \delta\gamma_y \end{pmatrix} \quad (2.6)$$

At each step of incremental strain, the formulation of the MSimpleDSS model defines the direction of incremental stress ratio,  $\delta\eta$ , to be in the direction between the incremental strain,  $\delta\gamma$ , and the direction computed from equation 2.6 with the magnitude given by equation 2.7:

$$\|\delta\eta\| = \left\| \left[ \frac{1}{\frac{1}{H} + \frac{1}{G_e}} \right] \delta\gamma \right\| \quad (2.7)$$

For uni-directional shearing where  $i = (1, 0)$ , the incremental stress-strain relationship from the MSimpleDSS model collapses to the one-dimensional formulation of the SimpleDSS model.

## 2.2. Modeling cyclic response

In order to describe the behavior of clays under multidirectional cyclic loading, a constitutive model needs to incorporate the effect of previous consolidation stress history and the accumulation of excess pore pressures and plastic strains as the number of cycles increases. The MSimpleDSS model

decouples the effective stress path and stress-strain response component to simplify the problem and allow for nearly independent determination of material parameters. The model considers cyclic loading as a sequence of monotonic steps where the stress state of a normally consolidated sample migrates inside the yield surface. Once inside the yield surface the soil behavior is closely related to the response of overconsolidated clay.

### 2.2.1. Pore pressure generation in cyclic loading

The effective stress path inside the PSS is controlled by a load state surface referred to as the Transitional State Surface (TSS). The MSimpleDSS model assumes that the orientation of the TSS is uniquely controlled by the shear stress ratio at last reversal point,  $\eta_{rev} = (\tau_{xrev}/\sigma_n, \tau_{yrev}/\sigma_n)$ , which is defined in stress space every time the stress state moves inside the current PSS or TSS. In other words, the orientation of the TSS simultaneously changes every time the reversal point is redefined. When the PSS is not activated the effective stress path can be described by the TSS as follows:

$$\eta \cdot \eta = \frac{\tan^2 \psi}{1 - \beta^m} - \left[ \frac{\tan^2 \psi}{1 - \beta^m} + \eta_{rev}^2 - 2\eta_{rev} \cdot \eta \right] \left( \frac{\sigma_n}{\sigma_{nrev}} \right)^B \quad \text{for } \|\eta\| < \tan \psi \quad (2.8)$$

$$B = \max\left(1, e^{-\theta(T_f - 0.09)}\right) \cdot m \quad (2.9)$$

$$T_f = \eta_{rev}^2 - \tan^2 \psi + (\tan^2 \psi + \eta_c^2 - 2\eta_{rev} \cdot \eta_c) \left[ \frac{\left( \frac{\sigma_n}{\sigma_{nrev}} \right)^m - (\beta - 0.15)^m}{1 - (\beta - 0.15)^m} \right] \quad (2.10)$$

Where parameter  $B$  is a function of relative distance from last reversal point to the strain-rate compatible PSS,  $T_f$  is the relative distance from last reversal point to the PSS, and  $\theta$  is a material parameter describing the effective stress path for cyclic loading. Eqn. 2.8 controls the positive generation of excess pore pressure and is valid only inside the PSS. Once the PSS is activated, continued shearing in the same direction will cause the state of stress to follow the PSS. If the PSS is activated at  $\|\eta\| < \tan \psi$ , continued shearing in the same direction will cause an increase in excess pore pressure whereas for  $\|\eta\| > \tan \psi$ , excess pore pressure will decrease (i.e., dilative response). In Eqn. 2.10 the PSS has been slightly modified to have the failure ratio  $(\beta - 0.15)$  account for the observed behavior of increasing rate of pore pressure generation when the state of stresses approaches the failure condition.

### 2.2.2. Accumulation of plastic strains

For simplicity, the model assumes that the stress-strain relationship under multi-directional shearing inside the PSS is independent between the  $x$  and  $y$  directions. This assumption is inferred from the observation of multidirectional shearing tests where soils inside the PSS behave more elastically. The stress-strain curve for states inside the PSS is, therefore, described by the one-dimensional formulation of Eqn. 6, in which the plastic modulus is determined independently in each direction.

$$\delta \eta_j = \left[ \frac{1}{\frac{1}{H_j} + \frac{1}{G_e}} \right] \delta \gamma_j \quad \text{where } j = (x, y) \quad (2.11)$$

$$H_j = \lambda \left[ 1 - \frac{\sin(\eta_j, \dot{\gamma}_j) \eta_j^2}{\Psi^2} \right] \left[ 1 - \frac{\max(\eta_{jrev})}{\Psi} \right] \times \left[ \Psi + \max(\eta_{jrev}) \right] \left[ \frac{\max\left(0.1, \left(1 - 4 \frac{\sigma_{jrev} - \sigma_n}{\sigma_p}\right)\right)}{\eta_j - \eta_{jrev}} \right] \quad (2.12)$$

$$\Psi = \frac{\tan \psi}{\sqrt{1 - \beta^m}} \quad (2.13)$$

Where  $\lambda$  is a material parameter controlling the accumulation of plastic strains inside the PSS. The reversal point for calculating plastic modulus in each direction is defined in strain space through a scalar strain amplitude parameter,  $\chi$ , as follows:

$$(\chi\dot{\chi})_j = \Delta\gamma_{jrev}\delta\gamma_j = \begin{cases} \geq 0 & \leftrightarrow \text{loading} \\ < 0 & \leftrightarrow \text{unloading; set reversal} \end{cases} \quad (2.14)$$

Where  $\Delta\gamma_{jrev} = \gamma_j - \gamma_{jrev}$  is the strain relative to the reversal point, and  $\delta\gamma_j$  is the incremental strain in each direction. Although the plastic stiffness is calculated by the reversal point defined in strain space, the shape of the TSS is determined from the reversal point defined in stress space.

### 3. DETERMINATION OF MATERIAL PARAMETERS

The MSimpleDSS model is characterized by seven input material parameters, five of which are necessary to describe the behavior of clay under monotonic loading, and two additional parameters that are required to describe the cyclic behavior. These parameters can be determined from one standard monotonic and one cyclic simple shear test respectively. The model was developed in a way that the material parameters describing the behavior under monotonic and cyclic loading can be determined independently.

#### 3.1. Monotonic material parameters

The first three parameters  $\psi$ ,  $\beta$ , and  $m$  control the shape of the PSS which defines the effective stress path during first loading from normally consolidated states and during yielding of the loading from overconsolidated states (Figure 3.1). Parameters  $G_n$  and  $G_p$  control the initial stiffness and shape of the stress-strain curve respectively (Figure 3.1). The model is formulated based on data from DSS tests in which the state of stresses are less than ideal boundary conditions when the shear strain is larger than 20-25% (Vucetic and Lacasse 1982; Airey and Wood 1987; DeGroot et al. 1994). Therefore, in this work, the large strain condition is defined as a shear strain of approximately 20%.

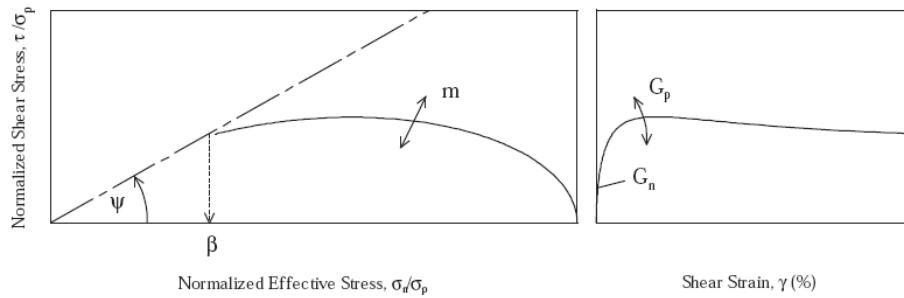
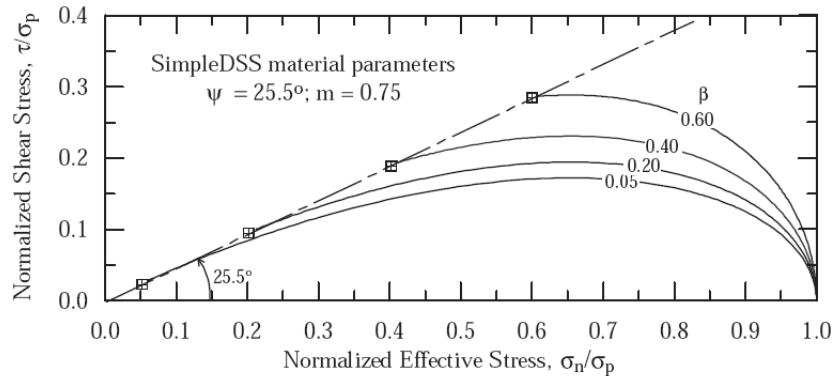


**Figure 3.1.** Monotonic parameters for undrained direct simple shear test (Biscontin, 2001)

Parameter  $\psi$  describes the maximum shear stress ratio ( $\tau/\sigma_n$ ) at large strains under both monotonic and cyclic shearing of normally consolidated clay. In the standard representation of the DSS test,  $\tan \psi$  is the slope of the failure envelope in the shear normal effective stress space (Figure 3.1). The value of  $\psi$  is found to be nearly constant for strains larger than 20%, therefore,  $\psi$  is chosen corresponding to a shear strain of 20%.

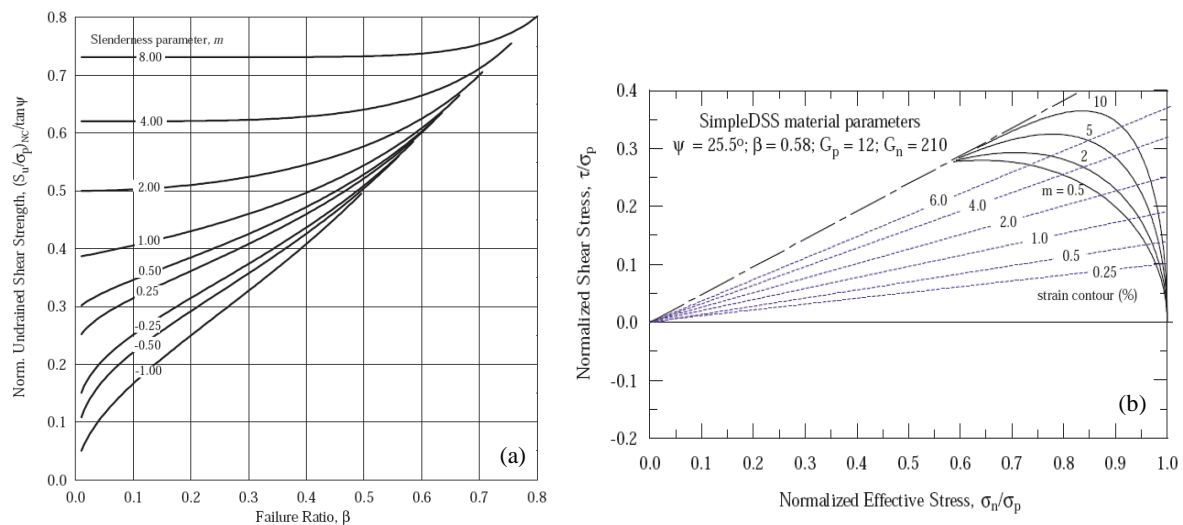
Parameter  $\beta$  describes the magnitude of excess pore pressure developed monotonically at large strain, and for a given value of  $\psi$ , it controls the shear strength,  $\tau_f$ , at large strains. Parameter  $\beta$  can be found directly from the inferred normalized effective stress path in a standard DSS test at a shear strain of approximately 20% (Figure 3.1). For a given slenderness parameter  $m$ , an increase in  $\beta$  causes not only an increase in shear strength at large strains but also an increase in the undrained shear strength. For modeling purposes, the undrained shear strength is controlled by adjusting the value of parameter

$m$ , as discussed below. Figure 3.2 illustrates the effect of parameter  $\beta$  on the predicted effective stress paths during monotonic DSS tests.



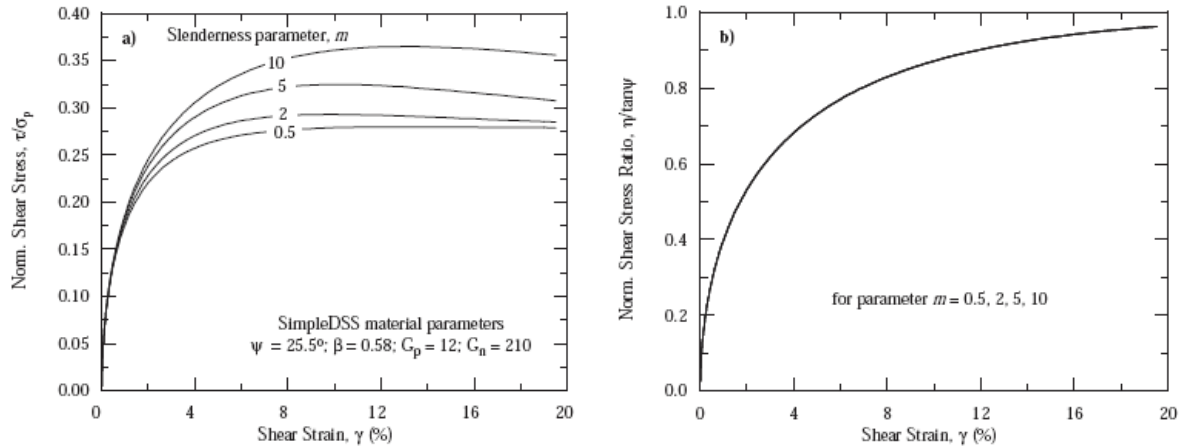
**Figure 3.2.** Effect of failure ratio parameter ( $\beta$ ) on the prediction of the effective stress paths during monotonic DSS tests for normally consolidated clay

Parameter  $m$  determines the size of the PSS, and thus it controls the magnitude of the undrained shear strength and the amount of excess pore pressure generated at the peak undrained shear strength. Parameter  $m$  can be obtained by a short parametric study to fit the effective stress path from a standard DSS test. Alternatively, it is possible to directly estimate parameter  $m$  by correlating it with the values of normalized undrained shear strength,  $S_u/\sigma_p$ , maximum obliquity,  $\tan \psi$ , and failure ratio,  $\beta$ , as shown in Figure 3.3a. Figure 3.3b illustrates the effect of the slenderness parameter  $m$  on the shape of the effective stress path for standard DSS tests. For a given value of  $\beta$ , an increase in parameter  $m$  increases the size of the PSS and the undrained shear strength while the excess pore pressure at peak shear stress decreases.



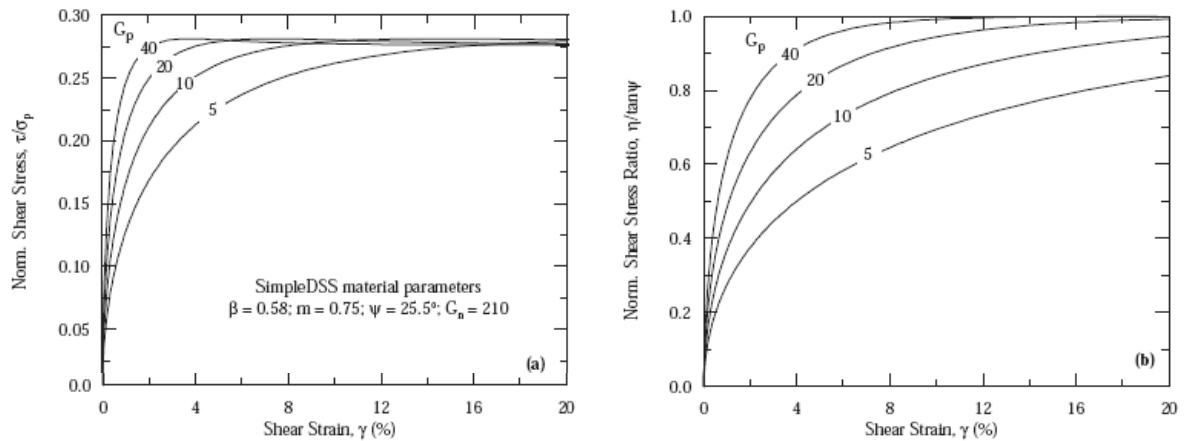
**Figure 3.3.** (a) Preliminary selection of parameter  $m$  based on the undrained shear strength from a standard DSS test (Pestana et al. 2000); (b) Effect of the slenderness parameter  $m$  on the prediction of the effective stress path during monotonic DSS tests for normally consolidated clay

Figure 3.4 illustrates that increasing parameter  $m$  causes an increase in the secant shear stiffness at all strain levels. However, if the relationships are plotted between strains and normalized shear stress ratio,  $\eta/\tan \psi$ , then every stress-strain curve collapses onto a unique curve independent of parameter  $m$  (Figure 3.4b). This is because the model is formulated such that by varying  $m$  and keeping all other material parameters constant, each strain contour on the effective normal and shear stress space has approximately a constant slope which intersects the x-axis at the origin, as shown in Figure 3.3b. This assumption is in excellent agreement with laboratory results.



**Figure 3.4.** Effect of slenderness parameter  $m$  on the prediction of stress strain characteristics during monotonic DSS tests for normally consolidated clays

Parameter  $G_p$  controls the shape of the stress-strain curve during first loading from a normally consolidated state. This parameter has no effect on the shape of the PSS. As shown in Figure 3.5, increasing the value of  $G_p$  increases the slope both in the normalized shear stress and normalized shear stress ratio versus shear strain spaces. As  $G_p$  increases, the soil becomes stiffer, the strain at failure decreases, and the magnitude of the peak undrained shear strength remains unchanged. Parameter  $G_p$  can be obtained directly by performing a small parametric study to match the normalized shear stress ratio versus shear strain curve from a standard (i.e.,  $\tau_c = 0$ ) DSS test. Although both parameters  $m$  and  $G_p$  affect the secant shear stiffness, parameter  $m$  has no effect on the shape of the stress-strain curve when plotted in the normalized shear stress ratio ( $\eta/\tan\psi$ ) space. Therefore, the factors that govern an increase in stiffness can be separated between the effects from the increase in undrained shear strength (i.e., effects from parameter  $m$ ) and the dependency on parameter  $G_p$ .



**Figure 3.5.** Effect of  $G_p$  on predicted stress-strain characteristics during undrained monotonic DSS tests

The material parameter  $G_n$  controls the initial stiffness of the loading and unloading portion of the stress-strain curve. This material parameter can be derived from insitu or laboratory shear wave velocity measurements. This parameter has a marked effect at the small strain level, and hence, the location of the  $G/G_{max}$  curve. However, it has a negligible effect on the shape of the stress-strain curve at higher shear strain levels (i.e.,  $\gamma > 1\%$ ). Therefore, the estimation of  $G_n$  can be simplified for modeling monotonic response since the behavior of interest is from intermediate to large shear strains. From the normalized stress-strain curve obtained during a standard DSS test, the normalized secant shear stiffness ( $G_{sec}/\sigma_p$ ) can be determined at each shear strain level by dividing the normalized shear stress ( $\tau/\sigma_p$ ) with its corresponding shear strain. These values of  $G_{sec}/\sigma_p$  are then plotted against shear strain in the log-log space. The value of  $G_n$  can then be estimated by projecting the curve back to a shear strain of about 0.001%. This strain is below the linear cyclic threshold shear strain,  $\gamma_{tl}$ , which

represents the limit of the value of small strain shear modulus,  $G_{max}$ , for cohesive soils at various plasticities (Vucetic 1994).

### 3.2. Cyclic material parameters

This section summarizes the selection of parameters  $\theta$  and  $\lambda$  and their influence on the prediction of stress-strain characteristics and pore pressure development of normally consolidated soils subjected to undrained cyclic loading.

Parameter  $\theta$  controls the rate of pore pressure generation during cyclic loading. This parameter can be derived from a cyclic DSS test by calibrating the rate of pore pressure generation as a function of the number of cycles. Figure 3.6 shows the effect of parameter  $\theta$  on the predicted development of pore pressure and accumulation of shear strain as a function of number of cycles. As parameter  $\theta$  increases, the rate of pore pressure generation decreases and the number of cycles to failure increases. However, cyclic shear strains at early stages of every test are very similar since they are mostly controlled by parameter  $\lambda$ .

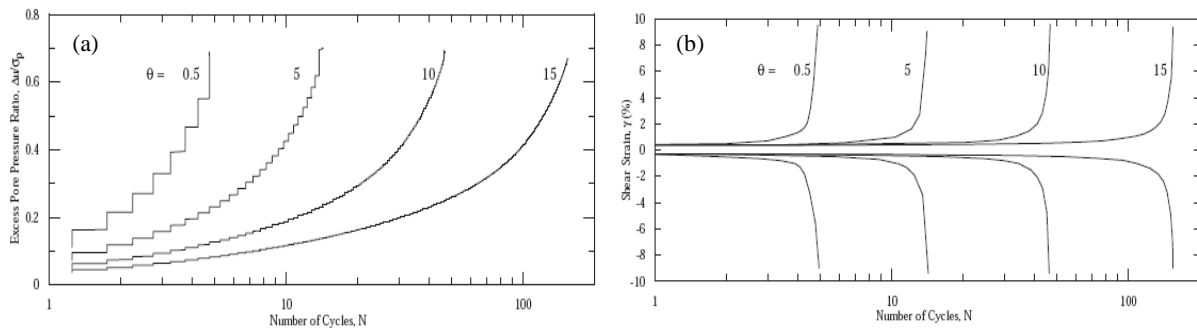


**Figure 3.6.** Effect of parameter  $\theta$  on the predicted development of pore pressure (a) and accumulation of shear strain (b) during undrained stress-controlled cyclic DSS tests with  $\tau_{cyc}/\sigma_p = 0.15$  and  $\tau_c = 0$

Parameter  $\lambda$  controls the magnitude of the plastic stiffness of soil inside the PSS and therefore describes the stiffness for soil that is sheared from an overconsolidated state. Moreover, it controls the shear stiffness and the plastic strain development as the number of cycles increases. Figure 3.7 shows the effect of parameter  $\lambda$  on the predicted maximum shear strain as a function of number of cycles for a symmetric stress-controlled cyclic DSS test with no consolidation shear stress (i.e.,  $\tau_c = 0$ ).

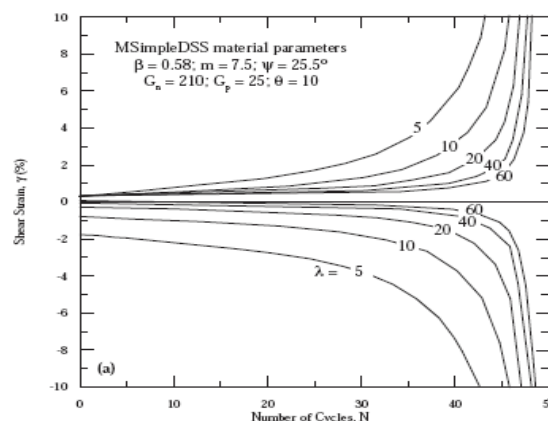


**Figure 3.7.** Effect of parameter  $\lambda$  on the predicted maximum cyclic shear strain during undrained stress controlled cyclic DSS tests with  $\tau_{cyc}/\sigma_p = 0.15$  and  $\tau_c = 0$

In addition, parameter  $\lambda$  determines the shape of the stress-strain curve and the magnitude of cyclic shear strain during each successive cyclic loading. During cyclic loading, the model assumes the soil to move on the PSS in the first quarter of cyclic shearing where its plastic stiffness is estimated from parameter  $G_p$ . As the stress reverses direction, the state of stress moves inside the PSS along the TSS

and the model uses parameter  $\lambda$  in computing the subsequent plastic stiffness. Therefore, parameter  $\lambda$  has the analogous meaning with parameter  $G_p$  but defined inside the PSS. Experimental data has shown that the ratio of  $G_p/\lambda$  is approximately 1 to 2.

#### 4. MODEL EVALUATION

To illustrate the model's capabilities, the authors compared experimental data from stress-controlled MDSS tests on San Francisco Young Bay Mud (YBM) from Biscontin (2001) with the predicted response. Soil samples were first loaded incrementally to reach a normally consolidated state under an applied shear stress ratio  $\eta_c = \{0, 0.2\}$ . The samples were then sheared at a strain rate of 5 %/hr under undrained stress-controlled conditions. Figure 4.1 shows the comparisons for various shearing directions with respect to the dip direction. From the figure it is apparent that the MSimpleDSS model is able to capture the effective stress and shear stress-shear strain paths of  $K_\alpha$  consolidated soil very well. Figure 4.2 compares the predicted response with the measured response of normally consolidated Boston Blue Clay (BBC) under cyclic DSS loading. It can be seen that the model is able to capture pore pressure generation and shear strain development with number of cycles very well.

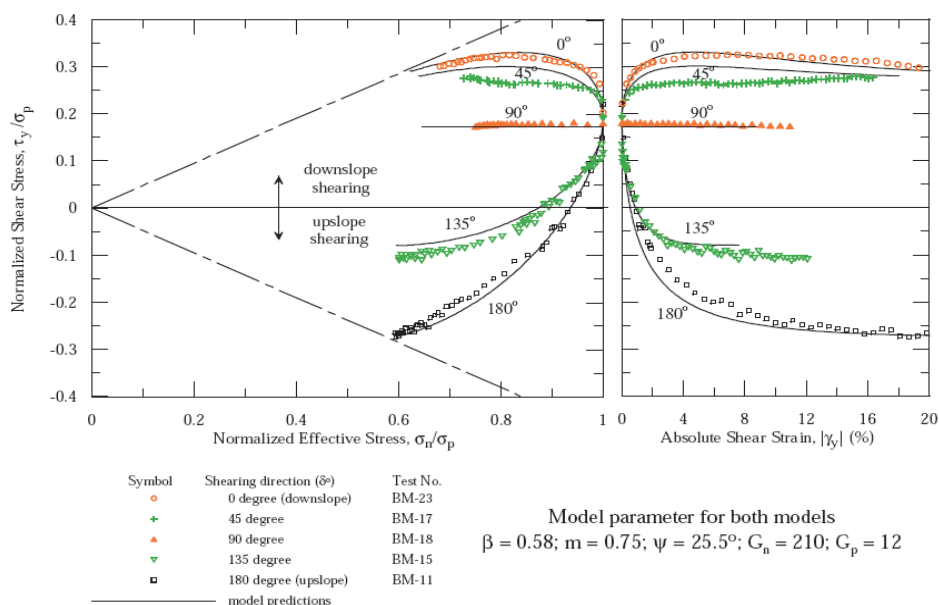


**Figure 4.1.** Effective stress paths and stress-strain curves in dip direction predicted by MSimpleDSS for MDSS tests on normally consolidated Young Bay Mud consolidated at  $\tau_c/\sigma_p = 0.2$ .

#### 5. CONCLUSION

The MSimpleDSS model is a modified version of the SimpleDSS model, and was developed to analyze the response of submarine slopes subjected to multidirectional seismic excitation. The model introduces several improved laws to better capture the stress redistribution and development of plastic strain and excess pore pressure during multidirectional shearing without introducing any additional parameters. To describe behavior under monotonic loading, the model requires five input material parameters which can be estimated from one standard DSS test. To describe the behavior of clay under cyclic loading the model requires two additional input material parameters that can be estimated from one stress-controlled cyclic DSS test.

The model is able to give good predictions of effective stress paths, stress-strain relationships, and undrained shear strengths under various directions of shearing for both stress and strain-controlled test conditions. The effect of strain rate can be taken into account by appropriately adjusting the material input parameters. This is discussed in Anantanavanich (2006).

The MSimpleDSS model has been implemented in the finite element code AMPLE2D, and numerical simulations were performed to determine the key factors that affect seismic response, such as earthquake motion characteristics, shear strain dependent stiffness and damping, thickness of soil profile, and consolidation stress history. The results of the numerical simulations are presented in a companion paper.

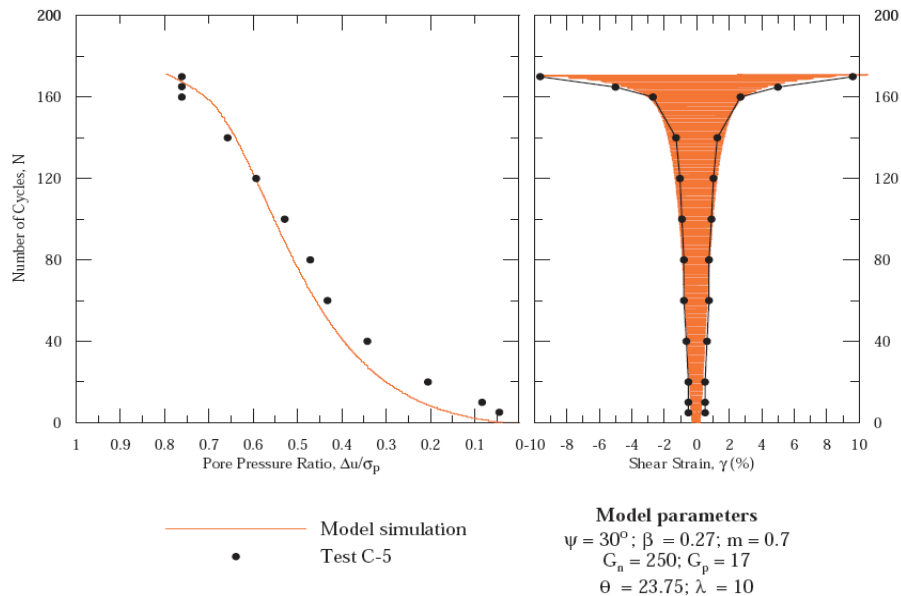


**Figure 4.2.** Measured data and model simulations for cyclic DSS tests on normally consolidated Boston Blue Clay,  $\tau_c = 0$ ,  $\tau_{cyc}/\sigma_p = 0.115$ , test data from Malek et al. (1987).

## ACKNOWLEDGEMENTS

This work was sponsored by the United States National Science Foundation.

## REFERENCES

- Airey, D. and D. Wood (1987). An evaluation of direct simple shear tests on clay. *Géotechnique* 37 (1), 25-35.
- Anantanavanich, T. (2006). Modeling the Rate Dependent Dynamic Response of Submarine Soft Clay Deposits. Ph. D. thesis, Dept. of Civil and Environmental Engineering, University of California, Berkeley
- Biscontin, G. (2001). Modeling the Dynamic Behavior of Lightly Overconsolidated Soil Deposits on Submerged Slopes. Ph. D. thesis, Dept. of Civil and Environmental Engineering, University of California, Berkeley.
- Boulanger, R., R. Seed, and C. Chan (1991). Effects of initial static driving shear stresses on the liquefaction behavior of saturated cohesionless soils. Geotechnical Engineering Research Report UCB/GT/91-01, Department of Civil and Environmental Engineering, University of California, Berkeley.
- Bugge, T., R. Belderson, and N. Kenyon (1988). The Storegga slide. *Philosophical Transaction of the Royal Society of London* 325, 357-388.
- DeGroot, D., J. Germaine, and C. Ladd (1994). Effect of nonuniform stresses on measured DSS stress-strain behavior. *Journal of Geotechnical Engineering* 120 (5), 892-912.
- Malek, A., A. Azzouz, M. Baligh and J. Germaine (1987). Undrained cyclic simple shear behavior of clay with application to pile foundations supporting tension leg platforms. MITSG 87-20, Massachusetts Institute of Technology, Cambridge, MA.
- Pestana, J., G. Biscontin, F. Nadim, and K. Andersen (2000). Modeling cyclic behavior of lightly overconsolidated clays in simple shear. *Soil Dynamics and Earthquake Engineering* 19, 501-519.
- Roscoe, K. and J. Burland (1968). On the generalized stress-strain behavior of wet clays. In *Engineering Plasticity*, 535-609. Cambridge University Press.
- Schofield, A. and C. Wroth (1968). *Critical State Soil Mechanics*. London: McGraw-Hill.
- Vucetic, M. (1994). Cyclic threshold shear strains in soils. *Journal of Geo. Eng.* 120 (12), 2208-2229.
- Vucetic, M. and S. Lacasse (1982). Specimen size effect in simple shear test. *Journal of Geo. Eng. Division* 108 (GT12), 1567-1585.